Process of magnetizing bulk amorphous alloys $Fe_{43+x}Co_{29-x}Y_8B_{20}$ (x=0 or 5)

To cite this article: M Nabialek *et al* 2019 *IOP Conf. Ser.: Mater. Sci. Eng.* **572** 012018

IOP Conf. Series: Materials Science and Engineering **572** (2019) 012018 doi:10.1088/1757-899X/572/1/012018

Process of magnetizing bulk amorphous alloys $Fe_{43+x}Co_{29-x}Y_8B_{20}$ (x= 0 or 5)

M Nabialek[1,*], B Jeż[1], K Jeż[1], P Pietrusiewicz[1], K Błoch[1], J Gondro[1], M M A B Abdullah[3] and A V Sandu[2]

[1]Institute of Physics, Faculty of Production Engineering and Materials Technology, Czestochowa University of Technology,19 Armii Krajowej Str., 42-200 Czestochowa, Poland

[2]Gheorghe Asachi Technical University of Iasi, Faculty of Materials Science and Engineering, 41 D. Mangeron Blvd., 70050, Iasi, Romania

[3]Geopolymer&Green Technology (CeGeoGTech), School of Material Engineering, Universiti Malaysia Perlis (UniMAP), 01000 Kangar, Perlis Malaysia

E-mail: bartek199.91@o2.pl

Abstract. The paper presents the results of investigations of the structure and magnetic properties of $Fe_{43+x}Co_{29-x}Y_8B_{20}$bulk amorphous alloys (x = 0 or 5). Alloy samples were made using injection a liquid alloy into a copper mold. The produced materials were characterized by soft magnetic properties, i.e. a high saturation of magnetisation value (about 1.15T) and a relatively low coercive field value (below 100 A/m). Increasing the cobalt content in alloys affected the high Curie temperature (around 700K). On the basis of H. Kronmüler's theory, an analysis of the magnetisation process in area so-called the approach to ferromagnetic saturation was carried out. The analysis showed that the impact on the process of magnetizing the produced materials have linear defects in the form of pseudo-dislocation dipoles.

1. Introduction

Bulk amorphous materials have been known for several decades. The main creator of the new group of materials is A. Inoue. On the basis of the trials conducted, A. Inoue developed three empirical principles as an indication during the production of bulk amorphous materials. Good glass ability is guaranteed by the negative heat of mixing of the alloy components, multi-component (at least three elements) and the large difference in the length of the atomic radius of the main alloy components [1, 2].

The application of these principles affects the increase in the viscosity of the liquid alloy. Higher viscosity prevents diffusion of atoms over further distances. Therefore, the lack of order of long-range atoms is typical for the amorphous structure. However, it is possible to create repetitive systems on a small scale in the volume of the alloy. Correctly created amorphous alloy is characterized by the lack of topological ordering with simultaneous occurrence of a certain degree of chemical ordering. Amorphous iron and cobalt based alloys exhibit the so-called good soft magnetic properties [3-9]. Co-based amorphous alloys have a very low coercive field value and relatively high saturation magnetization, while Fe-based alloys have a slightly higher coercive field value and higher saturation magnetization [10, 11]. In order to achieve the best properties, alloys containing both iron and cobalt

are developed. A known group of materials are amorphous alloys based on FeCoB characterized by relatively good magnetic properties [12,13].

An important factor affecting the magnetic properties of amorphous materials are defects in their volume. They occur in the form of point defects (free volumes) and line defects (pseudo dislocation dipoles) [14]. There is no direct method of observing these defects. However, it is possible to indirectly assess their quality and quantity. The magnetization vector is extremely sensitive to any imperfections in the structure. These defects force the rotation of the magnetization vector, hence it should be assumed that their presence affects the course of the primary magnetization curve [15, 16]. H. Kronmüller modified the Brown's micromagnetism theory and presented the following relationship describing magnetization:

$$\mu_0 M(H) = \mu_0 M_s \left[1 - \frac{a_{\frac{1}{2}}}{(\mu_0 H)^{\frac{1}{2}}} - \frac{a_1}{(\mu_0 H)^1} - \frac{a_2}{(\mu_0 H)^2}\right] + b(\mu_0 H)^{\frac{1}{2}} \quad (1)$$

Where: M_s – spontaneous magnetization, μ_0 – magnetic permeability of vacuum, H – magnetic field, a_i (i = ½, 1, 2) – angular coefficients of the linear fit, which correspond to the free volume and linear defects, b – slope of the linear fit corresponding to the thermally induced suppression of spin waves by a magnetic field of high intensity.

Elements in Equation 1 can be described as follows:

$$\frac{a_{1/2}}{(\mu_0 H)^{1/2}} = \mu_0 \frac{3}{20 A_{ex}} \left(\frac{1+r}{1-r}\right)^2 G^2 \lambda_s^2 (\Delta V)^2 N \left(\frac{2A_{ex}}{\mu_0 M_s}\right)^{1/2} \frac{1}{(\mu_0 H)^{1/2}} \quad (2)$$

$$\frac{a_1}{\mu_0 H} = 1{,}1\mu_0 \frac{G^2 \lambda_s^2}{(1-\nu)^2} \frac{N b_{eff}}{M_s A_{ex}} D_{dip}^2 \frac{1}{\mu_0 H} \quad (3)$$

$$\frac{a_2}{\mu_0 H^2} = 0{,}456\mu_0 \frac{G^2 \lambda_s^2}{(1-\nu)^2} \frac{N b_{eff}}{M_s^2} D_{dip}^2 \frac{1}{(\mu_0 H)^2} \quad (4)$$

Where: ΔV – means the change in volume due to the occurrence of a point defect characterized by a bulk density of N, A_{ex} – exchange constant, G – transverse elastic shear modulus, r – Poisson's ratio, λ_s – magnetostriction constant, D_{dip} – length of the linear defect, l_H – distance of exchange

Equation (2) describes the effect of point defects on the primary magnetization curve. Equations (3) and (4) describe the influence of linear defects of the structure on the magnetization process, the equation (3) concerns the condition $D_{dip} < l_H$, whereas the equation (4): $D_{dip} > l_H$ (4). For equations (4) $l_H$is the distance of at least two dipoles [17].

The area on the primary magnetization curve, where the magnetizing process is associated with the presence of defects in the structure is so-called area of approach to ferromagnetic saturation. Above this area, magnetization is related to the damping of thermally excited spin waves (Holstein-Primakoff paraprocess [18]). The stiffness parameter of the spin wave D_{spf} is associated with the parameter b, which can be described by the dependence:

$$b = 3{,}54 g\mu_0\mu_B \left(\frac{1}{4\pi D_{spf}}\right)^{3/2} kT(g\mu_B)^{1/2} \quad (5)$$

Where: k – Boltzman's constant, μ_B – Bohr magneton, g – gyromagnetic factor.

The aim of the study was to tested selected magnetic properties of bulk amorphous alloys with the chemical composition $Fe_{43+x}Co_{29-x}Y_8B_{20}$ (x = 0 or 5) and to analyze the course of the magnetization process in accordance with the theory of H. Kronmüller.

2. Methods and materials

The polycrystalline ingot was made in an arcing furnace with high purity elements (more than 99.9%). Elements was weighed with an accuracy of 0.0001 grams. The solidification process of the polycrystalline ingot was carried out in a protective atmosphere (Ar). In order to achieve the best degree of mixing of ingredients, the ingots were melted 7 times, each time inverting it to the other side. The melting temperature was regulated by change the current flowing through the electrode (180 - 380A). The solidification of the ingot was preceded each time by the melting of the titanium getter. The high affinity of titanium to oxygen ensures a high degree of purity of the atmosphere in the working chamber. 10-gram ingots made in this way were mechanically cleaned and divided into smaller pieces. The bulk amorphous alloy was produced using the method of injecting the liquid alloy into the copper mold [19-20, 22-28]. Production process was also carried out in a protective atmosphere of argon. The polycrystalline charge was placed in a quartz crucible. The ingot was melted using eddy currents. The molten material was injected into the copper mold under argon pressure.

Amorphous plates were subjected to mechanical cleaning and an ultrasonic cleaner. The produced materials were structural and selected magnetic properties research. The BRUCKER X-ray diffractometer, Advanced 8 model equipped with a CuKα lamp was used to determine the structure of the manufactured alloys. Samples were irradiated for 7 seconds per measuring step (0.02 °). The measurement was carried out for materials in the form of powder. Irradiation was carried out in the range of 30-100 ° angle 2Θ. Using the Faraday magnetic weight, the saturation magnetic polarization was measured and the Curie temperature of the alloys formed was determined. The measurement was carried out in the range from room temperature to 850K. By means of the LakeShore vibration magnetometer, primary magnetization curves and static magnetic hysteresis loops were measured. The measurement of the curves and loops was carried out to the intensity of the 2T magnetic field.

3. Research results

Figure 1 presents X-ray diffraction images for produced materials.

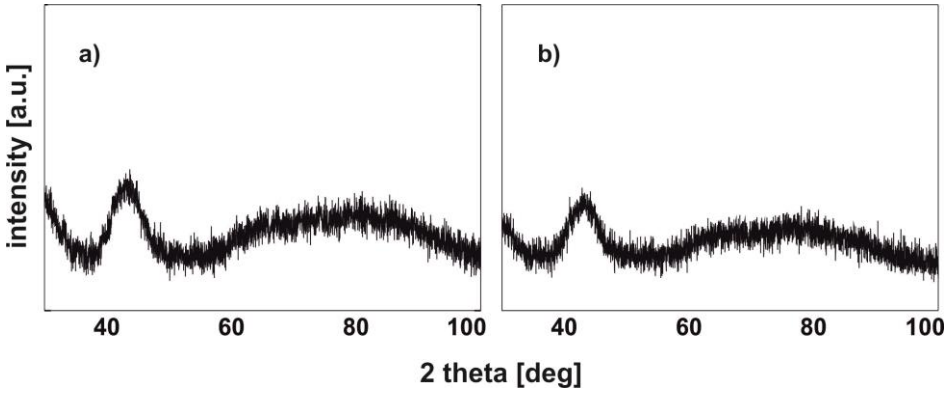

Figure 1. X-ray diffraction images for the alloy: a) $Fe_{43}Co_{29}Y_8B_{20}$, b) $Fe_{48}Co_{24}Y_8B_{20}$.

The recorded images are typical as for amorphous materials. Only broad maxima (in the range of 40° -50° 2 theta angle) from X-rays scattered on chaotically spaced atoms in the volume of the tested materials are visible on the diffractograms. Figure 2 presents reduced the saturation magnetic polarization curves as a function of temperature.

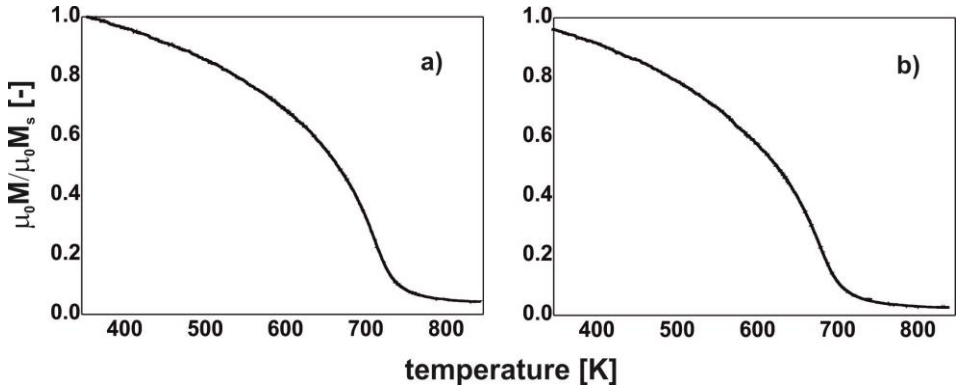

Figure 2. Reduced magnetic saturation polarization curves as a function of temperature for the alloy: a) $Fe_{43}Co_{29}Y_8B_{20}$, b) $Fe_{48}Co_{24}Y_8B_{20}$.

On curves (μ_0M/μ_0M_s) (T), gentle inflections from magnetic phase transition from ferro to paramagnetic state are visible. For alloys that meet the Heisenberg assumptions, it is possible to determine the Curie temperature using the critical coefficient $\beta = 0.36$. Figure 3 shows curves $(\mu_0M)^{1/\beta}$.

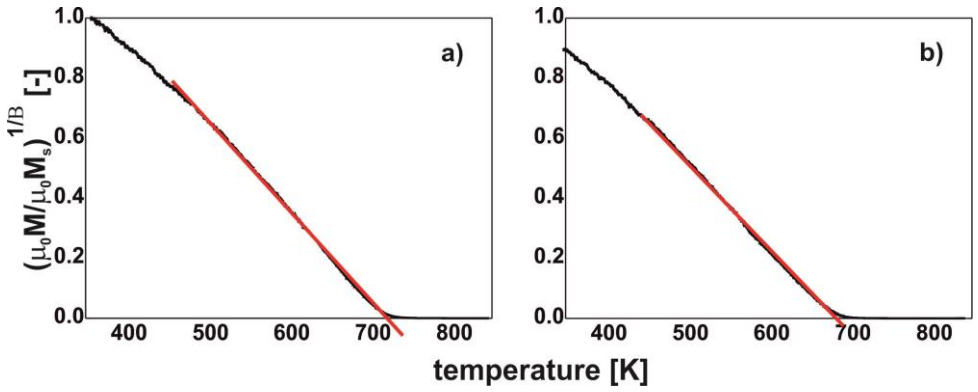

Figure 3. Reduced curves $(\mu_0M)^{1/\beta}$ for alloy: a) $Fe_{43}Co_{29}Y_8B_{20}$, b) $Fe_{48}Co_{24}Y_8B_{20}$.

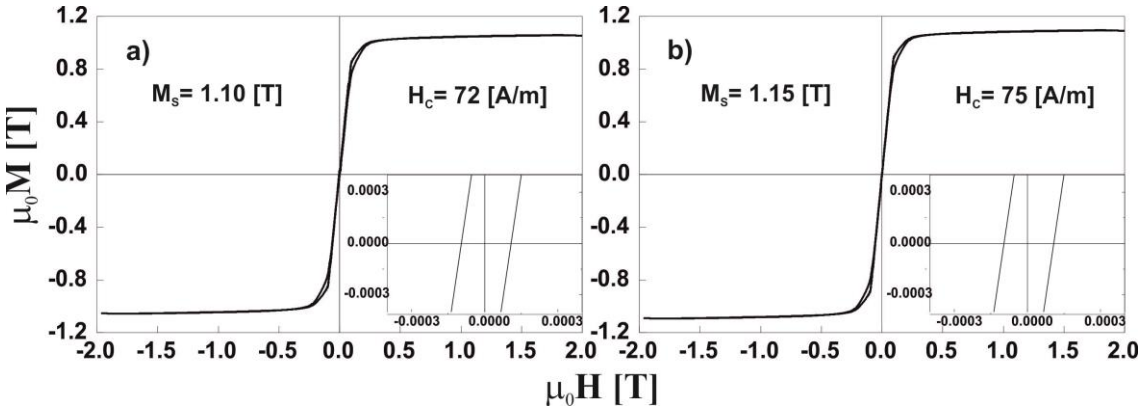

Figure 4. Static magnetic hysteresis loops for alloy a) $Fe_{43}Co_{29}Y_8B_{20}$, b) $Fe_{48}Co_{24}Y_8B_{20}$.

In the studied temperature range, for both tested alloys, there is one magnetic phase corresponding to the amorphous matrix (in accordance with the diffractograms, Figure 2). The $Fe_{43}Co_{29}Y_8B_{20}$ alloy has a Curie temperature of 710K while for the $Fe_{48}Co_{24}Y_8B_{20}$ alloy the transition temperature of the

amorphous matrix to the paramagnetic state is 675K. The temperature difference for the tested alloys is 35K which is related to the change in the Co content. The Curie temperature for iron is 1043K, while for cobalt it is 1388K, hence the reduction of the cobalt content in the alloy for iron results in a reduction of the Curie temperature of the amorphous matrix. Figure 4 presents static magnetic hysteresis loops for the produced materials.

The measurement was carried out in the range of external magnetic field strength up to 2T. The recorded curves are typical as for amorphous materials exhibiting so-called soft magnetic properties. The rectangular shape of the loop indicates a relatively easy course of magnetization of the manufactured alloys. The saturation of magnetization value for the $Fe_{43}Co_{29}Y_8B_{20}$ alloy is 1.10 T while for the $Fe_{48}Co_{24}Y_8B_{20}$ alloy it is 1.15 T. In contrast, the coercive field value for both alloys is about 75 A/m, which classifies the materials produced as soft magnetic [21]. Figure 5 presents the primary magnetization curves for the tested alloys.

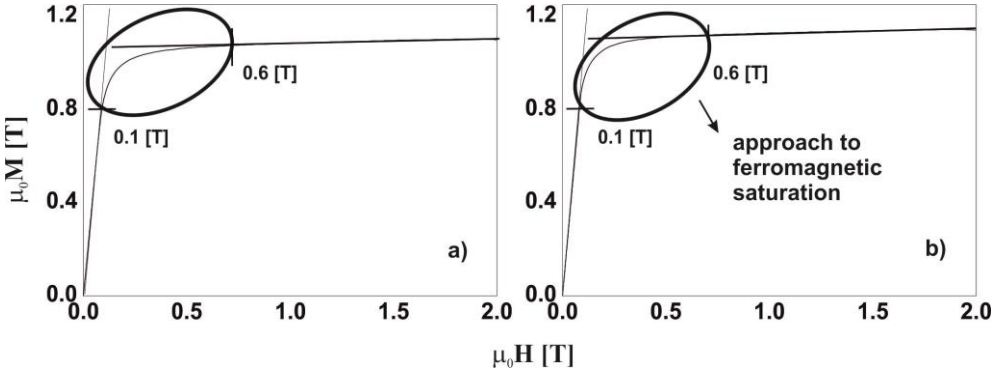

Figure 5. The primary magnetization curves for the alloy a) $Fe_{43}Co_{29}Y_8B_{20}$, b) $Fe_{48}Co_{24}Y_8B_{20}$.

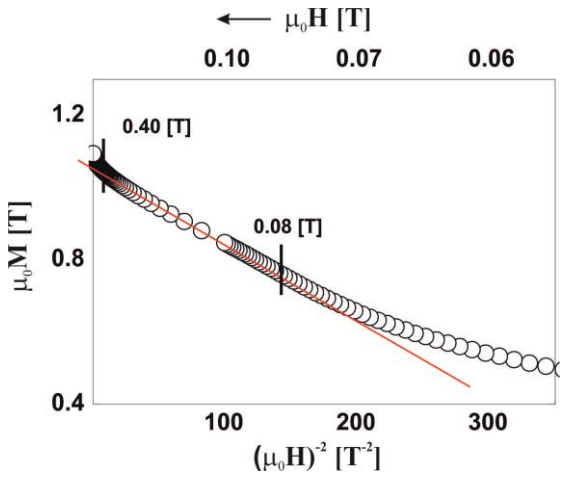

Figure 6. Analysis of the ferromagnetic saturation approach area for $Fe_{43}Co_{29}Y_8B_{20}$ alloy: dependence of $\mu_0M(\mu_0H)^{-2}$.

On the measured curves, an area so-called the approach to ferromagnetic saturation was pre-determined. According to the H Kronmüller theory, an analysis of this area was carried out (Figures 6 and 7). In the field of external magnetic field with an intensity of 0.08 - 0.40 T, the magnetizing process of the $Fe_{43}Co_{29}Y_8B_{20}$ alloy is associated with the rotation of the magnetization vector around linear defects of the structure that meet the dependence (4). This is indicated by the linearity of the function $\mu_0M(\mu_0H)^{-2}$ in the mentioned magnetic field strength range. Based on the analysis of the

primary magnetization curve for the $Fe_{48}Co_{24}Y_8B_{20}$ alloy, the presence of linear defects in the volume of the tested sample was identified. In the range of the external magnetic field from 0.09 to 0.15 T, the material magnetization process is related to the rotation of the magnetization vector around the linear defects that meet the dependence (3), whereas in the field strength range from 0.16 to 0.57 T, the magnetization is related to the presence of pseudo dislocation dipoles meeting the relationship (4) .

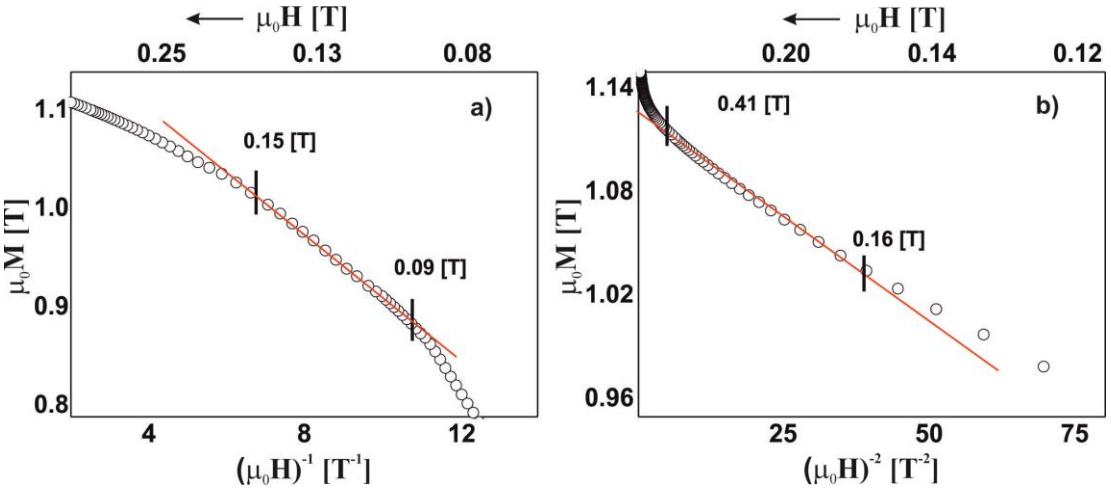

Figure 7. Analysis of the ferromagnetic saturation approach area for $Fe_{48}Co_{24}Y_8B_{20}$ alloy: a) dependence of $\mu_0M(\mu_0H)^{-1}$, b) dependence of $\mu_0M(\mu_0H)^{-2}$.

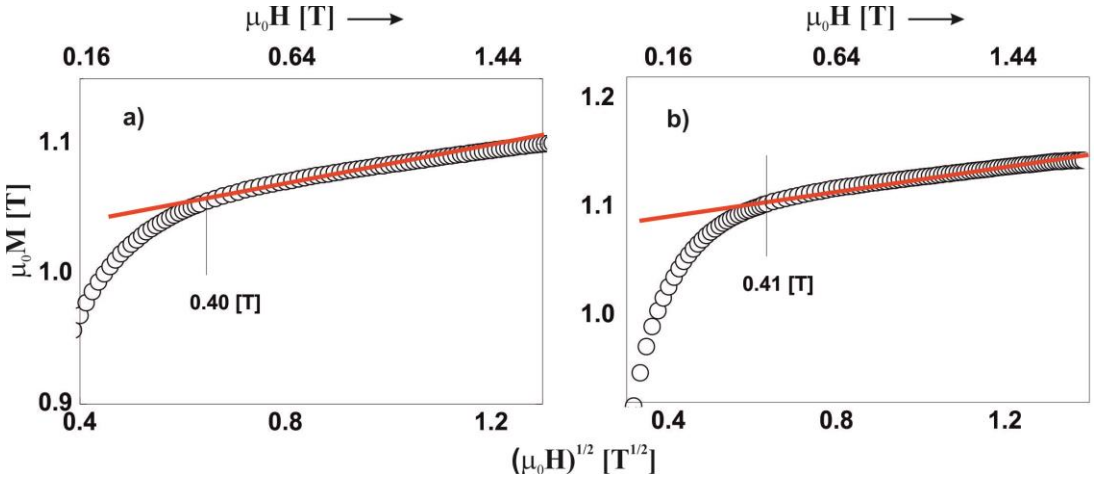

Figure 8. Dependence $\mu_0M(\mu_0H)^{1/2}$ for the alloy a) $Fe_{43}Co_{29}Y_8B_{20}$, b) $Fe_{48}Co_{24}Y_8B_{20}$.

Table 1. Magnetic properties of the alloy $Fe_{43+x}Co_{29-x}Y_8B_{20}$ (x= 0 lub 5).

	T_C [K]	M_S [T]	H_C [A/m]	Point defects	$D_{dip}<l_H$	$D_{dip}>l_H$	D_{spf} [meVnm^2]
$Fe_{43}Co_{29}Y_8B_{20}$	710	1.10	72	-	-	+	43
$Fe_{48}Co_{24}Y_8B_{20}$	675	1.15	75	-	+	+	48

Figure 8 presents an analysis of the magnetization process of the produced alloys in the external magnetic field above the approach to ferromagnetic saturation area. Above this area, the further process of magnetizing the material is associated with the damping of thermally excited spin waves. Holstein-Primakoff paraprocess describes dependence (5). As a result of its transformation, the spin

wave stiffness parameter D_{spf} can be determined. Table 1 presented the magnetic properties of the alloys tested.

The value of the parameter D_{spf} is related to the distance between the magnetic atoms in the sample volume. The increase in the D_{spf} parameter correlates with the increase in saturation of magnetization, which is the expected result.

4. Conclusions

The aim of the study was to determine the selected magnetic properties of bulk amorphous Fe-based alloys. An alloy with chemical composition $Fe_{43+x}Co_{29-x}Y_8B_{20}$ (x = 0 or 5) was produced by injection casting method. The obtained materials are characterized by so-called soft magnetic properties, i.e. high magnetization of saturation (~ 1.15T) and a relatively low coercive field value (~ 75 A / m). The high cobalt content in the produced alloys influenced the high Curie temperature (~ 700K). According to H. Kronmüller's theory, the primary magnetization curves were analyzed. Based on the numerical analysis of the curves, it was found that in both cases in the area so-called approach to ferromagnetic saturation, the magnetization process is related to the rotation of the magnetization vector around the linear defects. In volume of the $Fe_{43}Co_{24}Y_8B_{20}$ alloy, the presence of linear defects meeting the dependence of $D_{dip} > 1_H$ was identified. In contrast, the pseudo dislocation dipoles occurring in the $Fe_{48}Co_{24}Y_8B_{20}$ alloy are diversified in terms of dimensions, they meet the equation $D_{dip} > 1_H$ and $D_{dip} < 1_H$. This means that the process of solidifying the molten alloy was slightly different. The determined value of parameter D_{spf} is higher for the $Fe_{48}Co_{24}Y_8B_{20}$ alloy. This alloy also shows a slightly higher value magnetization of saturation, which is the expected result (an increase in iron content in the alloy at the expense of cobalt). However, taking into account all the values determined, it can be stated that the change of 5% cobalt to iron does not significantly affect the magnetic properties except for the lowering of the Curie temperature.

5. References

[1] Inoue A 2000 *Acta Materialia* **48** 279-306
[2] Inoue A, Kato A, Zhang T, Kim S G and Masumoto T 1991 *Materials Transaction JIM* **32** 609-616
[3] Inoue A, Kong F L, Han Y, Zhu S L, Churyumov A, Shalaan E and Al-Marzouki F 2018 *Journal of Alloys and Compounds* **731** 1303-1309
[4] Han Y, Chang C T, Zhu S L, Inoue A, Louzguine-Luzgin D V, Shalaan EandAl-Marzouki F 2014 *Intermetallics* **54** 169-175
[5] Dong C, Inoue A, Wang X H, Kong F L, Zanaeva E N, Wang F, Bazlov A I, Zhu S LandLi Q 2018 *Journal of Non-Crystalline Solids* **500** 173–180
[6] Li W, Yang Y Zand Xu J 2017, *Journal of Non-Crystalline Solids* **461** 93–97
[7] Kong F L, Chang C T, Inoue A, Shalaan EandAl-Marzouki F 2014 *Journal of Alloys and Compound*s **615** 163–166
[8] Kim S, Han B, Suhb J, Kim S, Kim D, Kim Y Kand Choi-Yim H 2017 *Intermetallics* **90** 164–168
[9] McHenry M E, Willard M A and Laughlin D E 1999 *Progress in Materials Science* **44** 291-433
[10] Kwon S, Kim Sand Choi-Yim H 2011 *Journal of the Korean Physical Society* **72(1)** 171-176
[11] Inoue A, Kong F L, Man Q K, Shen B L, Li R Wand Al-Marzouki F 2014 *Journal of Alloys and Compounds* **615** S2–S8
[12] Wang F, Inoue A, Han Y, Kong F L, Zhu S L, Shalaan E, Al-Marzouki FandObaid A 2017 *Journal of Alloys and Compounds* **711** 132-142
[13] Nabiałek MandJeż K 2018 *Revista de Chimie* **69(6)** 1593-1597
[14] Bloch Kand Nabialek M 2015 *Acta Physica Polonica A* **127** 442-444
[15] Kronmüller H, Fahnle M, Grimm H, Grimm Rand Groger B 1979 *J. Magn. Magn. Mater*. **13** 53
[16] Kronmüller H 1979 *IEEE Trans. Magn* **15** 1218

[17] Kronmüller H 2007 *General Micromagnetic Theory*, Handbook of Magnetism and Advanced Magnetic Materials, John Wiley&Sons **2** 703-739
[18] Holstein T and Primakoff H 1940 *Phys. Rev*. **58** 1098
[19] Nabiałek M 2015 *Journal of Alloys and Compounds* **642** 98–103
[20] Jeż B 2017 *Revista de Chimie* **68(8)** 1903-1907
[21] Liebermann H 1993 *Rapidly Solidified Alloys* New Jersey
[22] Minciuna M G, Vizureanu P, Achitei D C, Sandu A V, Berbecaru A and Sandu I G 2016 *Journal of optoelectronics and advanced materials* **18(1-2)** 174-178
[23] Bejinariu C, Burduhos-Nergis D P, Cimpoesu N, Bernevig-Sava A, Toma S L, Darabont D C and Baciu C 2019 *Quality-Access to Success* **20** 71-76
[24] Tóth L, Haraszti F and Kovács T 2018 *European Journal of Materials Science and Engineering* **3** 98-102
[25] Nabialek M and Jez K 2019 *European Journal of Materials Science and Engineering* **4** 23-28
[26] Berceanu C, Tarnita D and Filip D 2010 *Journal of the Solid State Phenomena, Robotics and Automation Systems,* **166** 45-50
[27] Tarnita D, Tarnita D N, Tarnita R, Berceanu C and Cismaru F 2010 *Materials Science and Engineering Technology, Special Edition Biomaterials* **41** 1070-1080
[28] Tarnita D, Catana M and Tarnita D N 2014 *Mechanisms and Machine Science* **20** 283-297